An Experimental and Analytical Investigation of Axisymmetric Diffusers

L. A. Povinelli*

NASA Lewis Research Center, Cleveland, Ohio

A finite-difference computer program for turbulent compressible flow was used to establish the performance of several diffuser shapes for experimental testing. The diffusers were designed to have a linear change in Mach number or a curvature fitted by a quadratic equation. Testing was performed with $M = 0.1$ to 0.9 with and without boundary-layer bleed. Above $M = 0.6$, data were obtained with a normal shock upstream of the diffuser entrance. Peak static pressure recovery occurred with a diffuser inlet $M = 0.75$. The quadratic diffuser yielded the highest total pressure recovery.

Nomenclature

L = diffuser length
M = Mach number
P = total pressure
ΔP = $P_{max} - P_{min}$
P_{ref} = facility reference pressure
p = static pressure
R = radius
ΔR = $R_C - R_H$
X = downstream distance; $X = 0$ is start of diffuser

Subscripts

1 = diffuser entrance
2 = diffuser exit
C = cowl
H = centerbody

Superscript

‾ = average values

Introduction

THE efficient performance of a supersonic inlet system is dependent on the proper design of the subsonic diffuser as well as the supersonic inlet portion. Although a considerable amount of effort has been directed toward the supersonic inlet, a relatively smaller effort has been devoted toward studying subsonic diffusers for advanced supersonic aircraft. Relatively few studies have been concerned with axisymmetric diffuser design.[1-4] One of those studies has discussed the possibility of improving supersonic inlet performance by the use of short subsonic diffusers.[4] Furthermore, little is known regarding the effects of boundary-layer bleed, inlet flow distortions, freestream turbulence, and vortex generators on axisymmetric diffuser performance.

This study is directed towards arriving at design criteria for axisymmetric diffusers for advanced supersonic aircraft. Specifically, the pressure recovery and minimum distortion were measured for several diffuser geometries and the results compared with the predictions from an viscid-inviscid computer program. The effects of boundary-layer bleed and vortex generators were also measured. Tests were conducted over a Mach number range of 0.1 to 0.9. Above Mach 0.6, a normal shock was present upstream of the diffuser inlet. The

Reynolds number for the tests was from 0.3×10^6 to 1×10^6 based on annulus height.

Analysis

Computational Method

The finite-difference procedure of Anderson[5] for turbulent, swirling, compressible flow in axisymmetric ducts was used to compute diffuser performance. The equations of motion are solved in a coordinate system made up of the streamlines and potential lines of the inviscid solution. Boundary-layer-type approximations are made in that coordinate system; the viscous effects being treated as perturbations on the flow. The analysis solves for the entire flow across the duct at each streamwise station. This strong interaction solution eliminates the matching problem resulting from inviscid flow merging with the boundary layer.

Diffuser Geometries

Performance calculations have been carried out for a series of axisymmetric diffusers and are presented in Ref. 6. Four different types of diffusers were chosen for investigation: a linear Mach number change, a linear area change, a linear pressure variation, and a quadratic area change. Only two of the four types analyzed in Ref. 6 were selected for this study. The first type selected was the linear Mach number change, or dM/dz diffuser, because it is representative of current designs. The dM/dz diffuser is characterized by gradual curvature at the entrance and low initial rates by diffusion. Maximum curvature and diffusion rate occur well downstream of the entrance, and the skin friction undergoes a relatively gradual decrease. The second type of diffuser selected for study was the quadratic area variation, that is, the wall contour was established by requiring the area distribution along the diffuser to be specified by a quadratic equation. This type of diffuser, which differs considerably from the dM/dz, is characterized by rapid diffusion and large wall curvature at the entrance and is similar to that studied by Stratford.[7] The skin friction drops very rapidly to a low but finite value. The proximity to zero skin friction coefficient makes the diffuser sensitive to flow disturbances or distortions and
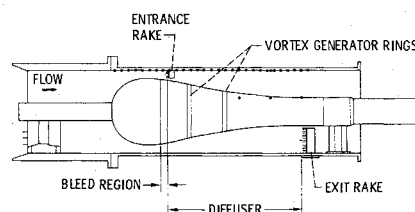

Fig. 1 Experimental diffuser apparatus.

may cause separation. However, the ability to operate successfully a diffuser of this type would lead to a given amount of diffusion in a minimum length provided the boundary layer does not grow too rapidly. High recoveries could, therefore, be accomplished in a shorter length than with other conventionally shaped diffusers. In this report the performance of the dM/dz and the Stratford (quadratic area variation) diffusers will be presented.

Apparatus and Procedure

General Approach

Testing was carried out using the apparatus shown in Fig. 1. Entering air was accelerated by the converging-diverging nozzle to supersonic velocity. The exhaust pressure was regulated so that a normal shock occurred in the divergent portion of the nozzle. The air then entered into the diffuser, where both the inlet and exhaust properties were measured in order to obtain performance data for the diffuser only.

Test Geometries

The diffuser geometry consisted of a straight cowl (12-in.-diam) and interchangeable centerbodies. Four centerbody shapes were tested and are shown in Fig. 2. The coordinates for the two diffusers are given in Table 1. The ratios of the diffuser length to the annular height (at the diffuser entrance) were 6 and 12. The entrance annular height was constant (1.5 in.) for all the geometries. The range of length to height ratios spans the range of subsonic axisymmetric diffusers tested on supersonic inlets at the NASA Lewis and Ames Research Centers. The diffuser exit-to-entrance area ratio was 2.0 for all geometries.

The removable centerbody was preceded by a short (2.3-in.-long) boundary-layer bleed section and the convergent-divergent nozzle (see Fig. 1). The bleed region had 600 holes drilled normal to the surface. The holes had an 0.067-in. diameter and were arranged in a staggered two-row pattern. The amount of bleed was variable from 0 to 3% of the inlet flow. The slope of the bleed section was 3°.

Test Conditions

Air was supplied at a maximum total pressure of 40 psig (35 lbs/sec) to the diffuser. The exit flow was removed by a 25-in. Hg vacuum (maximum) exhauster. The Reynolds number (based on annular height) was varied from 3×10^5 to 1×10^6. The range of Mach numbers at the diffuser entrance was varied from 0.1 to 0.9 (see Measurements section). Below a diffuser entrance Mach number of approximately 0.6, the flow was subsonic throughout the apparatus. Above 0.6, a normal shock (or shock train) was present in the divergent section of the nozzle or in the bleed region. The diffuser entrance Mach number was increased by reducing the back pressure. The reduction in back pressure also caused the shock location
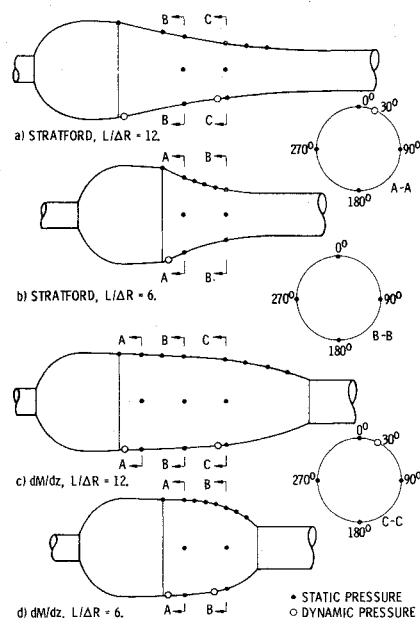

Fig. 2 Diffuser centerbody geometries.

to move farther downstream. At the highest Mach number used in this testing, the shock occurred in the bleed region. It is noted that the diffuser pressure recovery is defined in terms of the diffuser entrance and exit total pressures and does not take into account the pressure loss across the shock wave. Therefore, higher recovery does not necessarily mean higher pressure recovery at the compressor, particularly above Mach 0.625.

Measurements

An eight-tube rake at the diffuser entrance was used to measure seven total pressures equally spaced across the inlet annulus and the static pressure at the centerline of the annulus. Wall static pressures were measured every 1 in. along the cowl surface, from the nozzle to the diffuser exit. Circumferential static pressure measurements were also made on the cowl at 2, 6, and 10 in. downstream of the diffuser entrance. Wall static measurements were made on the centerbody as shown in Fig. 2. Dynamic pressure measurements were made at two locations on the centerbody surface. Circumferential static pressure measurements were made at 2 or 3 axial stations (see Fig. 2) on the diffuser centerbody surface. An exit rake was located either at the 9-in. or 18-in. location. The rake was composed of 14 total pressure tubes distributed across the annulus and a static pressure tube at the centerline of the annulus. Wall static pressures were measured on the centerbody and on the cowl at the same axial stations corresponding to the inlet and exit rakes. A linear interpolation was made with the two wall static pressure taps and the midstream static tube in order to obtain static pressures at the total pressure tube locations on the rake. These data then were used to determine local Mach numbers across the annulus. The local values then were area-weighted to yield area-weighted Mach numbers at the diffuser entrance and exit planes. The data presented in this report are plotted mainly as a function of the area-weighted diffuser-entrance Mach number or simply the diffuser-entrance Mach number. The data obtained at the inlet and exit rakes also were used to compute area-weighted pressure coefficients, static pressure rise, and total pressure recovery.

Vortex Generators

The diffuser geometries were tested with and without vortex generators. For the short diffuser, one row of generators was located approximately 1 in. downstream of the diffuser inlet. With the long diffusers the first row was at 0.8 in. for the

Table 1 Diffuser coordinates

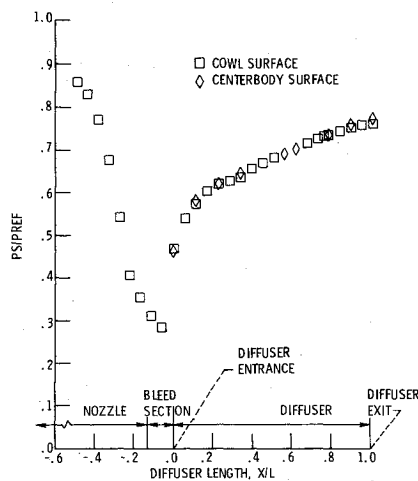| A) Linear Mach number change		B) Quadratic area variation	
X/L	R_H/R_C	X/L	R_H/R_C
0	0.750	0	0.750
0.1	0.745	0.1	0.692
0.2	0.737	0.2	0.636
0.3	0.726	0.3	0.583
0.4	0.711	0.4	0.532
0.5	0.692	0.5	0.484
0.6	0.665	0.6	0.442
0.7	0.629	0.7	0.405
0.8	0.577	0.8	0.378
0.9	0.497	0.9	0.360
1.0	0.354	1.0	0.354

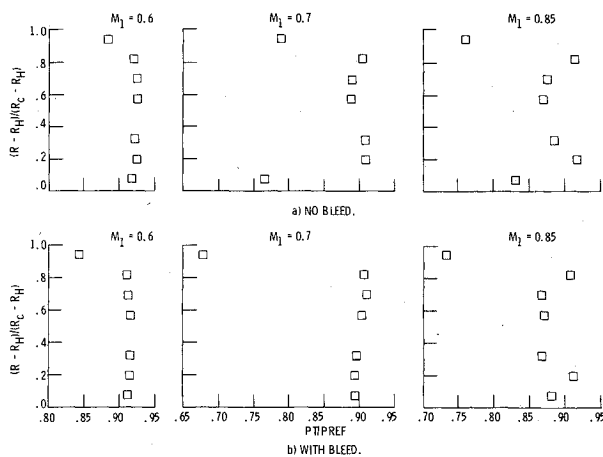Fig. 3 Static pressure distribution, dM/dz, $L/\Delta R = 12$, $M_I = 0.87$, no vortex generators, no bleed.

Fig. 4 Diffuser inlet pressure profiles.

Fig. 5 Total pressure recovery for long Stratford diffusers, $L/\Delta R = 12$, no vortex generators.
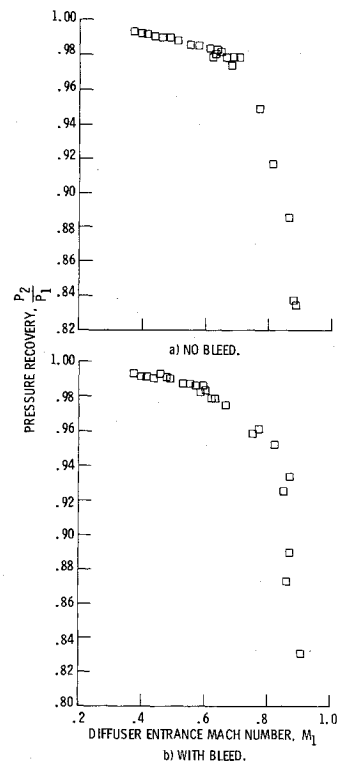
dM/dz diffuser and at 1.5 in. for the quadratic geometry. The second row was located 7.6 in. downstream of the diffuser inlet. The vortex generators had a chord- to-semispan ratio of 2. The generator cross section was equivalent to half of a NACA Series 0012 airfoil. The leading edge was rounded to have a 0.003 to 0.006-in. R leading edge. The generator chord length was 0.5 in. and the ratio of vortex generator spacing-to-chord length was nominally 1.7. The generators were oriented at 14° angle of attack and were in counter-rotating pattern.

Results

Static Pressure Distribution

A typical static pressure distribution through a section of the nozzle, bleed section, and the long dM/dz diffuser is shown in Fig. 3. The distribution starts just downstream of the convergence part of the centerbody and extends throughout the divergent nozzle section, the bleed section, and the diffuser as indicated in Fig. 3. The diffuser inlet station corresponds to an X/L value of 0 and extends to a value of 1. Figure 3 shows the distribution obtained with a diffuser entrance Mach number 0.847 as determined from the diffuser entrance pressure rake (see Measurements section). The pressure distribution shows that the flow is accelerated to supersonic velocities in the divergent section. A normal shock (or shock train) in the bleed region reduces the flow to subsonic velocity before entering the diffuser ($X/L = 0$). The static pressure rise then occurs in a continuous fashion through the diffuser.

Inlet Pressure Profiles

The total pressure profile measured by the rake at the diffuser entrance is shown in Fig. 4a. The inlet profile is shown for three values of the Mach number at the diffuser entrance. Distortion of the profile is seen to increase with Mach number as the shock system strengthens. This distortion is believed to be caused by the presence of a normal shock or shocks in the bleed region. Measurement of the pressure profile upstream of the nozzle (and upstream of the normal shock retention) showed uniform profiles at all of the test conditions. The effect of using a small amount of boundary-layer bleed (0.5 and 2% of the entrance flow at $M = 0.8$ and $M = 0.6$, respectively) on the centerbody (contoured surface of the diffuser) is shown in Fig. 4b. There is little effect of the bleed flow on the pressure profile at $M = 0.6$. However, at $M = 0.7$ the entire cross-stream profile is affected. The boundary layer on the centerbody surface is reduced greatly and the midstream profile is more uniform. At $M = 0.85$, the amount of bleed available was very small, and the effect on the profile is minimal. The results presented in the succeeding sections were, therefore, obtained with uniform inlet profiles up to $M = 0.6$-0.7. At $M = 0.7$-0.8, the profiles were very distorted in the absence of boundary-layer bleed, and at $M = 0.8$-0.9 the inlet flow was distorted with or without boundary-layer bleed.

Total Pressure Recovery – Long diffusers

The total pressure recovery for the long Stratford diffuser ($L/\Delta R = 12$) is shown in Fig. 5a. Excellent recovery was obtained from Mach 0.35 to 0.70 (98 to 99%). Above Mach 0.7, the recovery decreases very rapidly. Computer analysis of this diffuser indicated that the recovery would remain high over the entire Mach range tested, if the inlet profile were uniform. The entrance flow to the diffuser, however, becomes very distorted at the higher Mach numbers. The dropoff in recovery is believed to be because of the sensitivity of the diffuser to inlet flow distortions. The Stratford diffuser has a very rapid rate of diffusion immediately at the entrance. This rapid diffusion coupled with the onset of a normal shock (or shock train) makes the diffuser very sensitive to flow distortions, thereby increasing the susceptibility to flow separation. The effect of boundary-layer bleed on recovery is shown in Fig. 5b. An improvement in recovery is observed over the
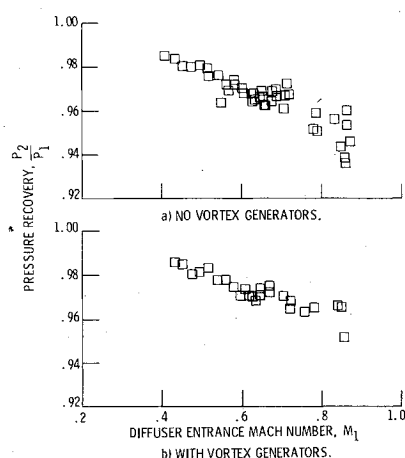
Fig. 6 Total pressure recovery for long dM/dz diffusers, $L/\Delta R = 12$, no bleed.
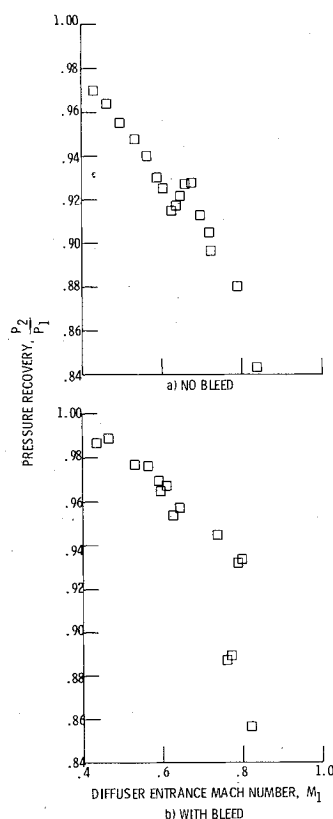

Fig. 7 Total pressure recovery for short Stratford diffusers, $L/\Delta R = 12$, no vortex generators.

Fig. 8 Total pressure recovery for short dM/dz diffusers, $L/\Delta R = 6$, no bleed.

range from $M = 0.75$ to $M = 0.85$. As seen in Fig. 4, the bleed flow caused the inlet profile to become more uniform at $M = 0.7$ whereas, the limited bleed at $M = 0.85$ did not cause much change. Hence, the recovery of the diffuser, which is very sensitive to inlet distortions, increased in a corresponding fashion. Installation of a row of vortex generators at the upstream location did not improve the recovery. The lack of improvement is because the generators could not be located sufficiently far upstream for the vortices to energize the boundary layer before separation, which probably occurred at the sharp corner.

The pressure recovery for the long dM/dz diffuser is shown in Fig. 6a. The same general trend is observed in the recovery behavior as with the Stratford diffuser. However, the values of the recovery are lower up to a Mach number of 0.75. A crossover occurs at that point and the dM/dz diffuser exhibits better performance than the Stratford. Hence, the sensitivity of the dM/dz geometry make it relatively insensitive to the inlet flow distortions. Indeed, the use of bleed did not have a
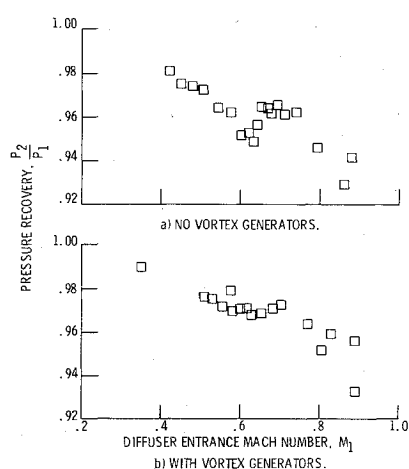
significant influence on recovery. Computer analysis showed that the dM/dz diffuser would have lower recovery than the Stratford diffuser over the entire Mach range tested. This behavior was verified by the results above up to Mach 0.75. The analysis for the dM/dz geometry also indicated flow separation at a point near the diffuser exit, where the centerbody has a rapid final curvature. One, therefore, would expect vortex generators to be effective, if located sufficiently far upstream. The experimental results with a row of vortex generators in the upstream location improved the recovery 0.5 to 0.75% (see Fig. 6b). The results obtained show the same qualitative trends as those in Ref. 11 for low speed (150 fps) two-dimensional diffusers, that is, geometries with rapid initial diffusion rates yield higher recovery but have greater sensitivity.

An additional feature was observed in the recovery curves. At a Mach number of approximately 0.625, a normal shock occurs upstream of the diffuser inlet. A slight rise in recovery is observed at that condition. This increase may result from a reduced skin friction coefficient in the region of the normal shock. Matthews et al.[8] have analyzed wake function. The results (see Fig. 1 of Ref. 8) show that the integrated skin friction coefficient over the region where the shock affects the boundary layer is less than the skin friction coefficient with an undisturbed boundary layer. The reduction in skin friction coefficient leads to lower shear stress at the wall and higher total pressure recovery.

Pressure Recovery – Short Diffusers

Computer analysis indicated that flow separation would occur close to the entrance of the short Stratford diffuser ($L/\Delta R = 6$). Hence, the use of boundary-layer bleed might be expected to prevent separation. The use of vortex generators, on the other hand, would not be expected to be helpful due to an insufficient path length to enable the vortices to energize the low momentum boundary layer. The experimental results in Fig. 7 bear out the expectations. The recovery is generally low (Fig. 7a), no bleed, no generators) and is very sensitive to inlet flow distortions. Boundary-layer bleed improved the performance appreciably (Fig. 7b) by allowing the flow to remain attached at the diffuser entrance. However, the diffuser is still quite sensitive to distortions at the higher Mach numbers. The effect of shock boundary-layer interaction on skin friction is readily apparent at $M = 0.625$ in Fig. 7a.

The results for the short dM/dz diffuser ($L/\Delta R = 6$) are shown in Fig. 8a. The pressure recovery is generally 1 to 2% lower than that obtained with the longer geometry ($L/\Delta R = 12$). Use of the computer analysis indicated that separation would occur near the exit of the diffuser ($X/L \approx 0.9$). Hence, locating vortex generators near the diffuser entrance should introduce sufficient mixing to prevent separation. The ex-
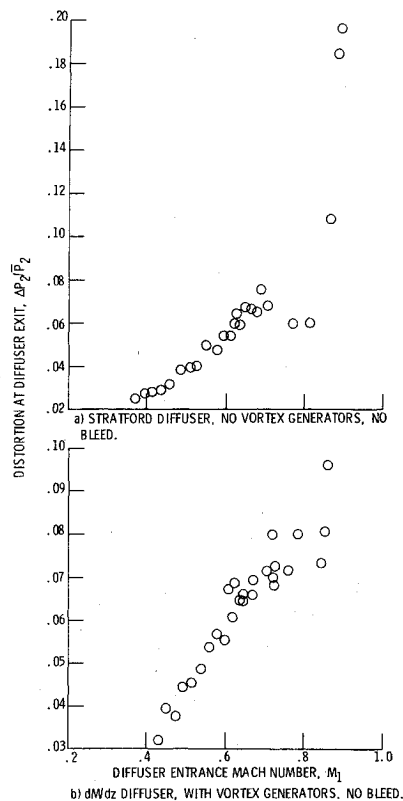
Fig. 9   Total pressure distortion at diffuser exit station for long diffusers, $L/\Delta R = 12$.

Fig. 10   Total pressure distortion at diffuser exit station for short diffusers, $L/\Delta R = 6$.

perimental results show that the generators doe enhance the performance; (see Fig. 8b). The recovery with generators is within 0.25 to 0.5% of those obtained with the larger dM/dz diffuser ($L/\Delta R = 12$) over the entire Mach number range. The short dM/dz diffuser also is insensitive to distortions in the entrance flow. Therefore, a reduction in diffuser length by a factor of 2 does not appear to degrade the diffuser's performance. The rise in pressure recovery when the normal shock occurs in the throat region ($M = 0.625$), is seen in Fig. 8a. As mentioned previously, this rise is attributed to skin friction reduction. From the results of Matthews,[8] it appears as if skin friction is reduced when the boundary layer is thickened. Use of bleed therefore, should decrease boundary-layer thickness, yielding higher friction losses and poorer recovery, provided that separation was not occurring previously. The experimental results with bleed show that, indeed, the recovery is 0.5 to 1% lower than the no-bleed results. It is noted further that bleed is generally ineffective with the dM/dz diffuser because the gradual curvature and lack of a high diffusion rate allow for the development of a healthy boundary layer. As indicated earlier, higher diffuser recovery does not necessarily mean higher pressure at the compressor face.

Distortion

The long diffusers yielded distortion values (i.e., $\Delta P_2/\bar{P}_2$) that were 7% at $M = 0.7$, as shown in Fig. 9a and b. The data for the short diffusers are given in Fig. 10a for the quadratic and 10b for the dM/dz. At $M = 0.7$, the distortion is 15% for the quadratic and 12% for the dM/dz diffuser.

Comparison with Computational Analysis

Figure 11a shows a comparison of the experimental results for the dM/dz diffuser and the computer analysis. The experimentally measured total pressure profiles at the diffuser entrance were used as input for the computations. The computer results show a rise in recovery at an entrance Mach number of approximately 0.62, corresponding to the experimental
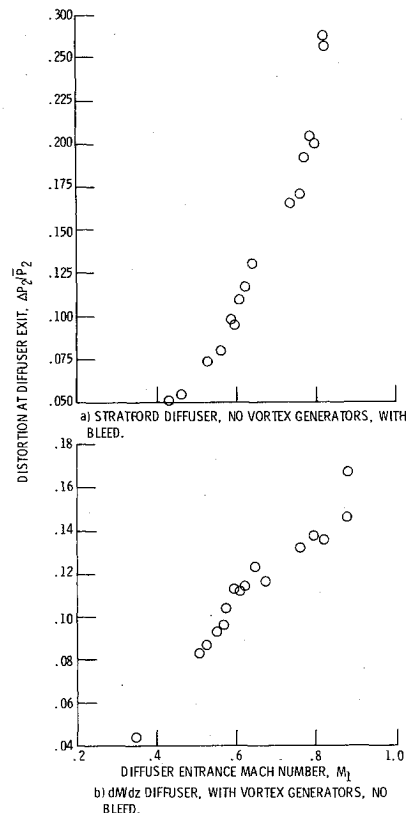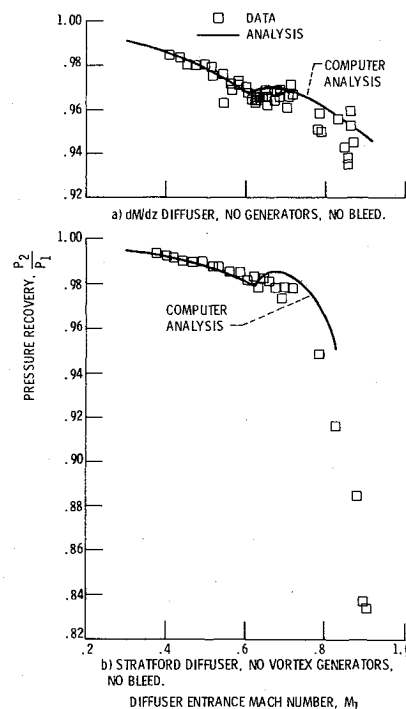

Fig. 11   Comparison of experimental data and numerical computation, $L/\Delta R = 12$.

results. This rise in recovery is more discernable in Figs. 6-8. The increase in pressure recovery is believed to be associated with the increased blockage (thicker boundary layer), leading to a reduction in skin friction coefficient. Figure 11b compares the results for the long quadratic diffuser. Again, the experimental pressure profiles at the diffuser entrance were used as starting conditions for the numerical calculations. The

experimental results and the computations show reasonably good agreement over the Mach number range.

Conclusions

The results from this study have shown that diffuser length-to-height ratios of 12 tend to be very conservative in design. The highest total pressure recovery, up to an entrance Mach number of 0.75, was obtained with a Stratford diffuser ($L/\Delta R = 12$). At a Mach number of 0.7, the recovery was 98% and the total pressure distortion at the diffuser exit was 7%. The long dM/dz diffuser ($L/\Delta R = 12$) had a slightly lower recovery; being 97% at Mach 0.7 with a distortion of 7%. The dM/dz diffuser, however, was less sensitive than the Stratford diffuser to the distortions present in the entrance flow at the higher Mach numbers (0.75 to 0.9). The increased sensitivity of the Stratford diffuser is caused by a combination of the rapid divergence at the entrance and the effect of the upstream normal shock on the behavior of the boundary layer.

A reduction of 50% in the length of dM/dz diffuser ($L/\Delta R = 6$) did not cause any significant reduction in the performance. At Mach 0.7, the pressure recovery was 97%; the distortion was 12%, and the diffuser was insensitive to entrance flow distortions. Therefore, for a slight increase in distortion level, one can obtain comparable recovery with half the length. The short Stratford diffuser yielded less favorable results. The recovery was the lowest (95.5% at $M = 0.7$) and the distortion was the highest (15%).

The experimentally obtained pressure profiles at the diffuser entrance were used as input conditions for a viscid/inviscid diffuser program. Good agreement was obtained between the numerical computations and the experimental data for the long diffusers. Use of the analysis for the short diffusers indicated where flow separation would occur, thereby providing information for the location of vortex generators.

References

[1] Wasserbauer, J. F., Shaw, R. J., and Neumann, H. E., "Design of a Very-Low-Bleed Mach 2.5 Mixed-Compression Inlet with 45 Percent Internal Contraction," TM X-3135, Mar. 1975, NASA.

[2] Sorensen, N. E. and Smeltzer, D. B., "Investigation of a Large-Scale Mixed-Compression Axisymmetric Inlet System Capable of High Performance at Mach Numbers 0.6 to 3.0," TM X-1507, Feb. 1968, NASA.

[3] Sovran, G. and Klomp, E. D., "Experimentally Determined Optimum Geometries for Rectilinear Diffusers with Rectangular, Conical or Annular Cross-Section," *Fluid Mechanics of Internal Flow*, edited by G. Souran, Elsevier Publ., 1967, pp. 270-312.

[4] Sorensen, N. E. and Bencze, D. P., "Possibilities for Improved Supersonic Inlet Performance," *Journal of Aircraft*, Vol. 11, May 1974, pp. 288-293.

[5] Anderson, O. L., "Finite-Difference Solution for Turbulent Swirling Compressible Flow in Axisymmetric Ducts with Struts," CR-2365, Feb. 1974, NASA.

[6] Povinelli, L. A. and Anderson, B. H., "A Computer Analysis of Subsonic Diffuser Design," Proposed NASA Technical Memorandum, 1977.

[7] Stratford, B. S., "An Experimental Flow with Zero Skin Friction Throughout its Region of Pressure Rise," *Journal of Fluid Mechanics*, Vol. 5, Jan. 1959, pp. 17-35.

[8] Matthews, D. C., Childs, M. E., and Paynter, G. C., "Use of Coles' Universal Wake Function for Compressible Turbulent Boundary Layer," *Journal of Aircraft*, Vol. 7, March-April 1970, pp. 137-140.

[9] Seddon, J., "The Flow Produced by Interaction of a Turbulent Boundary Layer with a Normal Shock of Strength to Cause Separation," ARC-R&M-3502, 1967, Aeronautical Research Council, Great Britain.

[10] Coles, D., "The Law of the Wake in the Turbulent Boundary Layer," *Journal of Fluid Mechanics*, Vol. 1, Pt. 2, July 1956, pp. 191-226.

[11] Carlson, J. J., Johnston, J. P., and Sagi, C. J., "Effects of Wall Shape on Flow Regimes and Performance in Straight, Two-Dimensional Diffusers," *Transactions of ASME Journal of Basic Engineering*, Vol. 89, Mar. 1967, pp. 151-160.